HAL open science

Bone morphogenetic protein 9 regulates early lymphatic-specified endothelial cell expansion during mouse embryonic stem cell differentiation

Mariela Subileau, Galina Merdzhanova, Delphine Ciais, Véronique Collin-Faure, Jean-Jacques Feige, Sabine Bailly, Daniel Vittet

To cite this version:

Mariela Subileau, Galina Merdzhanova, Delphine Ciais, Véronique Collin-Faure, Jean-Jacques Feige, et al.. Bone morphogenetic protein 9 regulates early lymphatic-specified endothelial cell expansion during mouse embryonic stem cell differentiation. Stem Cell Reports, 2019, 12 (1), pp.98-111. 10.1016/j.stemcr.2018.11.024 . hal-03206209

HAL Id: hal-03206209

https://hal.science/hal-03206209

Submitted on 21 Oct 2021

HAL is a multi-disciplinary open access archive for the deposit and dissemination of scientific research documents, whether they are published or not. The documents may come from teaching and research institutions in France or abroad, or from public or private research centers.

L'archive ouverte pluridisciplinaire **HAL**, est destinée au dépôt et à la diffusion de documents scientifiques de niveau recherche, publiés ou non, émanant des établissements d'enseignement et de recherche français ou étrangers, des laboratoires publics ou privés.

Distributed under a Creative Commons Attribution - NonCommercial 4.0 International License

Version of Record: https://www.sciencedirect.com/science/article/pii/S2213671118304934
Manuscript_1992a2f349e8d1a22b9bb9eab6ade149

Bone Morphogenetic Protein 9 regulates early lymphatic-specified endothelial cells expansion during mouse embryonic stem cell differentiation.

Mariela SUBILEAU[1], Galina MERDZHANOVA[1], Delphine CIAIS[1,2], Véronique COLLIN-FAURE[1], Jean-Jacques FEIGE[1], Sabine BAILLY[1], Daniel VITTET[1].

[1]Univ. Grenoble Alpes, Inserm, CEA, BIG-BCI, 38000 Grenoble, France;

[2] present address: Univ. Côte d'Azur, CNRS, Inserm, iBV, 06189 Nice, France

Contact: daniel.vittet@cea.fr

Running title: BMP9 expands lymphatic-specified endothelial cells

© 2018 published by Elsevier. This manuscript is made available under the CC BY NC user license
https://creativecommons.org/licenses/by-nc/4.0/

Summary:

Exogenous cues involved in the regulation of the initials steps of lymphatic endothelial development remain largely unknown. We have used an *in vitro* model based on the co-culture of vascular precursors derived from mouse ES (embryonic stem) cell differentiation and OP9 stromal cells to examine the first steps of lymphatic specification and expansion. We found that Bone Morphogenetic protein 9 (BMP9) induced a dose-dependent biphasic effect on ES cell-derived vascular precursors. At low concentrations, below 1 ng/mL, BMP9 expands the LYVE-1-positive lymphatic progeny and activates the calcineurin phosphatase/NFATc1 signaling pathway. In contrast, higher BMP9 concentrations, preferentially enhance the formation of LYVE-1-negative endothelial cells. This effect results from an OP9 stromal cell-mediated VEGF-A secretion. RNA silencing experiments indicate specific involvement of ALK1 and ALK2 receptors in these different BMP9 responses. BMP9 at low concentrations may be a useful tool to generate lymphatic endothelial cells from stem cells for cell replacement strategies.

Highlights:

-Low doses of BMP9 raise lymphvasculogenesis during ES cell differentiation.

-NFATc1 signaling operates in BMP9-induced lymphatic endothelial cells expansion.

-High doses of BMP9 increase LYVE-1-negative endothelial cells formation.

-A specific differential involvement of ALK1 and ALK2 mediates the BMP9 effects

Introduction:

The lymphatic vascular system is essential for immune surveillance and for the regulation of interstitial tissue fluid homeostasis. Defects in lymphatic development and/or dysfunction of lymphatic vessels are associated with the pathogenesis of several diseases (Aspelund et al., 2016). In particular, lymphatic vascular insufficiency can lead to lymphedema, a disabling disorder characterized by lymphatic fluid stasis and tissue swelling, mostly affecting the extremities (Jiang et al., 2018). Secondary lymphedema is commonly observed after surgery and radiotherapy of breast cancer. Although first-line decongestive and, in more severe cases, surgical therapies have proven useful to reduce edema, no efficient curative treatment currently exists (Shaitelman et al., 2015). Microsurgical lymphatic reconstruction procedures such as lymphatic venous anastomosis and vascularized lymph node transfer are other therapeutic options for the management of lymphedema, but some complications may occasionally develop (Shaitelman et al., 2015). Another promising approach would be to regenerate the damaged lymphatic vasculature by cell-based therapies (Qi and Pan, 2015). Embryonic and tissue stem cells have been postulated to be interesting sources of lymphatic derivatives that could be useful for cell replacement and lymphatic regeneration (Lee et al., 2015; Qi and Pan, 2015; Toyserkani et al., 2015). Several signaling pathways and molecular factors involved in lymphatic vessel development and lymphangiogenesis have been identified. However, the factors involved in the regulation of the initiation of lymphatic vessel development remain poorly characterized.

In the mouse embryo, until very recently, the dogma was that the lymphatic system is mainly originating from embryonic veins. Several studies have indeed shown that lymphatic specification could be observed since E9.5 in a subset of cells in the wall of the cardinal vein. These cells started to express PROX-1, under the control of COUP-TFII and SOX18 (for review, see (Semo et al., 2016)). Further lymphatic differentiation and lymph sac morphogenesis, occurring under the control of

VEGF-C stimulation`, was observable at E11.5. A role for NFATc1 has also been postulated during these processes, this transcription factor being expressed in endothelial cells undergoing lymphatic fate specification and in lymphatic cells constituting the primary lymph sacs (Kulkarni et al., 2009). Although the veins constitute an important source of lymphatic endothelial cell progenitors, the existence of non-venous sources that can contribute to the development of lymphatic vessels has now also been established for a significant part of the dermal, the mesenteric and the heart lymphatic vasculature (for review see (Kazenwadel and Harvey, 2016; Ma and Oliver, 2017)). The inductive signals and extracellular factors controlling lymphatic cell fate specification during embryonic development remain poorly characterized. Only few regulatory pathways have been identified to date (for review, see (Semo et al., 2016)). Both retinoic acid and ERK signaling have been established as positive regulators of the transcriptional program leading to lymphatic differentiation from the venous vasculature in the mouse embryo (for review, see (Semo et al., 2016)). Such an effect is also reported for WNT5B, described as an inducer of lymphatic cell fate in both zebrafish and human ES cells (for review, see (Semo et al., 2016)). In contrast, NOTCH signaling and the proangiogenic BMP2 have been identified as negative regulators of lymphatic specification (Dunworth et al., 2014; Murtomaki et al., 2013).

Mouse embryonic stem (ES) cell differentiation has been previously demonstrated to constitute a useful tool to identify molecular pathways involved in vascular development. Indeed, the early steps of vascular differentiation are recapitulated by this model (for review, see (Jakobsson et al., 2007)). Moreover, it has also been characterized that the earliest stages of lymphatic development can be observed during mouse ES cell differentiation either in embryoid bodies (Kreuger et al., 2006; Liersch et al., 2006) or during co-culture of ES-derived vascular progenitors on murine OP9 stromal cells (Kono et al., 2006; Vittet et al., 2012).

Bone morphogenetic proteins (BMPs), which have been characterized as essential factors for early embryonic development and stem cell fate (Sieber et al., 2009) appear as good candidates to exert a

role in the early lymphatic differentiation process. Some BMPs have emerged as potent regulators of vascular development and/or angiogenesis (Goumans et al., 2018). Except the inhibitory BMP2 effect reported above (Dunworth et al., 2014), whose action was postulated to be mediated by PROX-1 inhibition, the potential effects of BMPs on lymphatic development have not been addressed to date. While BMP9 was originally described as a potent osteogenic factor (Lamplot et al., 2013), it has also recently been found to influence lymphangiogenesis, lymphatic collecting vessel maturation and valve morphogenesis (Levet et al., 2013; Yoshimatsu et al., 2013). In addition, BMP9 was also found to be involved in the regulation of lymphatic endothelial cell proliferation and endothelial cell plasticity (Yoshimatsu et al., 2013).

In this study, we have investigated the potential role of BMP9 in early lymphatic development using the mouse ES cell *in vitro* differentiation model, in order to better characterize the initial events governing the expansion of the lymphatic endothelial lineage.

Results:

Early steps of lymphatic differentiation take place during co-cultures of ES-derived FLK-1+ vascular precursors on OP9 stromal cells.

We first performed a series of experiments to confirm and further provide evidence that the *in vitro* experimental differentiation model we used, mimics the initial differentiation commitment into the lymphatic endothelial cell lineage. The main steps of the procedure and treatments are illustrated on Figure 1A. As shown on Figure 1B, cell clusters exhibiting an endothelial morphology are obtained from co-cultures of FLK-1+ vascular precursors and OP9 stromal cells. Immunofluorescence staining experiments of these co-cultures revealed that endothelial-like cell clusters are mostly constituted by CD31+ and LYVE-1+ expressing cells. In parallel, the presence of scattered and/or cord-like organized CD31+ LYVE-1- cells was observed (Figure 1C and 1D). During the first days in co-culture, LYVE-1

expression, previously reported as an indicator of lymphatic endothelial competence, appeared to initiate in a subset of cells that were first expressing CD31 and which seemed to further expand (Figure S1). At day 10 of differentiation, we and others have previously shown that CD31+ LYVE-1+ cells represented a cell population that is committed early towards the lymphatic endothelial lineage (Kono et al., 2006; Vittet et al., 2012). The lymphatic lineage commitment of LYVE-1-positive cells is further supported by the expression of PROX-1, a marker of the endothelial lymphatic identity. PROX-1 expression in LYVE-1-positive cells was detected both by immunofluorescence staining (Figure 1, E to G), and by quantitative RT-PCR experiments (Figure 1, H to I). Unexpectedly, CD31+ LYVE-1- cells were also displaying a *Prox-1* expression (Figure 1, H to I), that might correspond to a putative early differentiation step preceding the LYVE-1 expression differentiation stage.

BMP9 expands ES-derived CD31+ LYVE-1+ early lymphatic-specified endothelial cell population.

We then asked whether BMP9 could affect lymphatic endothelial differentiation from FLK-1-positive ES-derived vascular precursors. ES-derived FLK-1-positive vascular precursors were co-cultured on OP9 stromal cells for 24 hours before treatment in the presence of different concentrations of the tested agents for another period of 4 days. Quantitative flow cytometry analysis showed that BMP9 exerted a bell-shaped dose-dependent effect on the formation of LYVE-1-positive cells, eliciting a 2-fold increase over control. A peak in the percentage of LYVE-1-positive cells was observed at 0.3 ng/mL, while at 10 ng/mL, the BMP9 response was similar to the untreated control (Figure 2A). Consistent with this analysis, we noticed that the formation of LYVE-1-positive endothelial sheet-like cell clusters were larger after treatment with 0.3 ng/mL BMP9 (Figure S2). Interestingly, BMP10, which is the closest member to BMP9 (Garcia de Vinuesa et al., 2016), gave a similar profile response (Figure 2A). In contrast, at similar concentrations, BMP2 did not increase the formation of LYVE-1-positive cells whereas at 50 ng/mL, it significantly inhibited this process (Figure 2A).

Another series of experiments, depicted in Figure 2B, was performed to characterize the kinetics of the BMP9 effect and to determine if the BMP9-induced increase in LYVE-1-positive cell population was resulting from the activation of a proliferation process. After a single BMP9 addition at day 6, a significant increase in the LYVE-1+ cell population was only observed beyond day 8 (Figure 2C). BrdU incorporation studies with pulse labeling of the cells in co-culture at day 7 or at day 8 revealed that BMP9 significantly activated the proliferation of the LYVE-1-positive cell population at day 8, eliciting more than a 1.5 fold rise over control (Figure 2D). Such an increase in BrdU incorporation in response to BMP9 was not observed at day 7.

BMP9 activates FLK-1+ vascular precursors and interferes with the calcineurin/NFATc1 signaling pathway.

The canonical BMP signaling pathway downstream of type I receptors leads to the phosphorylation of SMAD1/5 proteins. We then investigated the effect of the addition of 0.1 ng/mL BMP9, a dose in the range of those inducing LYVE-1-positive cell formation, on SMAD1/5 phosphorylation in FLK-1-positive sorted vascular precursors. A high SMAD1/5 phosphorylation level was obtained in response to 0.1 ng/mL BMP9 in FLK-1-positive sorted vascular precursors at day 5, but not in OP9 cells (Figure S3). These observations are consistent with a functional coupling of BMP9 with phosphorylation of SMAD1/5 proteins on FLK-1-positive cells, which could activate the initial stages of the differentiation process leading to the further expansion of the endothelial lymphatic lineage.

We next investigated whether BMP9 regulates the expression of transcription factors (COUP-TFII, SOX18 and PROX-1) known to be involved in the commitment and the early differentiation into the lymphatic endothelial cell lineage (for review, see (Ma and Oliver, 2017; Semo et al., 2016)). We measured by quantitative RT-PCR their expression levels after a 24h stimulation by 0.3 ng/mL BMP9. As a positive control of the efficiency of the BMP9 treatment, we looked at the expression level of *Smad6* that has been shown to be induced by BMP9 in primary lymphatic endothelial cells culture

(Niessen et al., 2010). The expressions of *Coup-tfII, Sox18* and *Prox-1* in vascular progenitors were unchanged after BMP9 stimulation (Figure 3A). Moreover, no significant variation in *Prox-1* expression was observed after 4 hours of BMP9 stimulation on FLK-1+ vascular precursors (data not shown). This time point was investigated since a BMP9-induced transient regulation of *Prox-1* expression, which lasted only a few hours, was reported in previous studies performed on adult lymphatic endothelial cells (Levet et al., 2013; Yoshimatsu et al., 2013).

We also investigated whether the transcription factor NFATc1, that has been established to be involved in lymphatic vascular development (Kulkarni et al., 2009), could be a target for BMP9. We found that *Nfatc1* gene expression was slightly but significantly induced, in response to 24 hours stimulation to 0.3 ng/mL BMP9, in ES cell-derived vascular derivatives in co-culture with OP9 stromal cells (Figure 3A). The calcineurin phosphatase/NFATc1 signaling pathway as a target for BMP9 was further confirmed at the protein level on FLK-1+ vascular precursors. As illustrated on figure 3B, a higher NFATc1 protein level was measured after 20 min stimulation with 0.3 ng/mL BMP9.

Moreover, to demonstrate that calcineurin-NFATc1 signaling may be involved in the control of LYVE-1-positive cell formation induced by low doses of BMP9, we performed the experiments in the presence of cyclosporin A, an inhibitor of calcineurin phosphatase activity and thereby of NFATc1 signaling (Horsley and Pavlath, 2002). We observed that cyclosporin A significantly inhibits BMP9-induced LYVE-1 positive endothelial cell expansion, further supporting a role of NFATc1 in the response elicited by BMP9 (Figure 3C).

High concentrations of BMP9 direct ES-derived vascular progenitor differentiation towards LYVE-1-negative endothelial cells through potential involvement of VEGF-A.

Since a previous work reported that 1 ng/mL BMP9 can regulate endothelial cell fate of mature endothelial cells (Yoshimatsu et al., 2013), we then wondered whether the decrease in LYVE-1-

positive cell formation towards basal control level, observed after the treatment with high BMP9 concentrations (Figure 2A), could reflect a preferential commitment towards another endothelial lineage or another endothelial cell differentiation stage. We found that BMP9, at concentrations above 0.5 ng/mL, significantly increased in a dose-dependent manner the formation of CD31+ LYVE-1- cells (Figure 4A and 4B). This effect was not observed for BMP10 or BMP2 (Figure 4A).

A recent study described the induction of VEGF-A synthesis and secretion in mesenchymal stem cells in response to BMP9 (Ai et al., 2015). A constitutive *Vegf-A* expression by OP9 stromal cells has also been reported and was found to be enhanced when ES-derived endothelial cells were co-cultured with OP9 cells (Matsumura et al., 2003). We therefore wondered whether the induction of CD31+ LYVE-1- endothelial cell formation observed at high BMP9 concentrations could be mediated by VEGF-A. First, we tested the effects of VEGF-A addition in the co-cultures of FLK-1-positive vascular precursors and OP9 stromal cells. As reported in Figure 5A, we observed a dose-dependent induction of the formation of CD31+ LYVE-1- cells in response to VEGF-A. Interestingly, this differentiation occurred at the expense of the LYVE-1-positive cell population since an inhibition of the formation of LYVE-1-positive cells was found in parallel (Figure 5A). Although a VEGFA-induced proliferative effect may probably also contribute to the CD31+ LYVE-1- cell rise, a major VEGFA effect was seen on the endothelial cell repartition between the two cell populations, without significant variations in the total number of endothelial cells (Figure 5B).

We next investigated whether the effects of BMP9 (10 ng/mL) could be mediated through VEGF-A, and we analyzed by ELISA the presence of VEGF-A in the supernatant of ES-derived FLK-1+ cells co-cultured on OP9. We found that VEGF-A was secreted at low levels during the co-culture of ES-derived precursors on OP9 stromal cells (Figure 5C) and that BMP9 treatment at 10 ng/mL significantly induced VEGF-A secretion, rising near a two-fold increase. The involvement of VEGF-A in the BMP9 response was supported by the use of VEGF-A neutralizing antibodies in the co-culture differentiation protocol, that inhibited the BMP9-induced formation of CD31+ LYVE-1- cells (Figure

5D). As a control, this antibody was observed to partially block the CD31+ LYVE-1- cell differentiation response induced by the addition of human recombinant VEGF-A (data not shown). In order to identify the cellular origin of VEGF-A induced by BMP9 in the culture medium, we made the hypothesis that OP9 stromal cells could constitute a potential source. We first investigated a potential BMP9 functional coupling with phosphorylation of SMAD1/5 proteins in OP9 cells at high BMP9 concentrations. OP9 cells were serum-starved for 1 hour before stimulation with or without BMP9. We found a marked SMAD1/5 phosphorylation in response to treatment with 10 ng/mL BMP9 for 1 hour (Figure 5E). We also observed that BMP9 induces a 2-fold increase in VEGF-A secretion by OP9 stromal cells after 48 hours of stimulation (Figure 5F).

Differential involvement of BMP9 type I receptors in CD31+ LYVE-1- and CD31+ LYVE-1+ cell populations formation from ES-derived vascular precursors in co-culture with OP9 stromal cells.

We then wondered whether the different specific responses elicited by low and high BMP9 concentrations may be the result of differential receptor mobilization. Two Type I receptors are currently described activated by BMP9: ALK1 and ALK2 (for review see: (Garcia de Vinuesa et al., 2016; Goumans et al., 2018)). We found a major *Alk1* mRNA expression level against *Alk2* in FLK-1+ cells (Figure S4A) On the other hand, a predominant *Alk2* mRNA expression was observed in OP9 cells compared to *Alk1* which remained barely expressed. (Figure S4A). We then performed RNA silencing experiments and first checked knock-down efficiencies at the time points post-transfection when cells were stimulated by BMP9 (Figure S4B and S4C).

Lymphatic endothelial cell development in response to 0.3 ng/mL BMP9 was then examined, after siRNA transfection either in FLK-1+ precursor cells or in both precursors and OP9 cells. We found that the BMP9-induced LYVE-1-positive cell formation was partially but significantly inhibited after *Alk1* silencing but was not affected by *Alk2* knockdown (Figure 6A). On the other hand, we found that, when RNA silencing was done in OP9 cells, the knockdown of *Alk2* prevented the increase in the

formation of CD31+ LYVE-1- endothelial cells induced by high BMP9 concentrations in the co-cultures of FLK-1+ vascular precursors on these OP9 transfected cells (Figure 6B). We also observed in parallel, that *Alk2* silencing in OP9 cells blocked SMAD1/5 phosphorylation and VEGF-A secretion induced by 10 ng/mL BMP9, whereas *Alk1* silencing did not interfere with these responses (Figure 6C and 6D).

Discussion:

In this study, we found that BMP9 increases the expansion of LYVE-1-positive early lymphatic-specified endothelial cells during mouse embryonic stem cell differentiation in a bell-shaped dose-dependent manner. At low doses, BMP9 increases the formation of LYVE-1-positive endothelial cell derivatives, at least in part via the calcineurin phosphatase/NFATc1 signaling pathway. In contrast, high BMP9 doses, by promoting in addition the VEGF-A secretion by OP9 cells, result in the induction of LYVE-1-negative endothelial cell formation. RNA silencing experiments indicate specific involvement of distinct type I BMP receptor subtypes in these different BMP9 effects. We also provide further evidence for *Vegf-A* gene expression being a target of high BMP9 concentrations in stromal cells. A hypothetical model recapitulating our data is illustrated on Figure 7.

Previous *in vitro* studies have reported BMP9 effects on differentiated ES-derived blood endothelial cells and/or mature blood endothelial cells (David et al., 2007; Rostama et al., 2015; Scharpfenecker et al., 2007; Suzuki et al., 2010). Both positive and negative effects on cell proliferation and/or migration were described, strongly suggesting a cell context- and dose-dependent effect for BMP9 regulation. In *in vivo* angiogenesis models, BMP9 mostly appears as a vascular endothelial quiescence factor (for review see (Cunha et al., 2017)). In this study, we show that BMP9 is also involved in the regulation of the early processes governing LYVE-1-positive lymphatic-specified endothelial cell formation.

Since we previously established a negative effect of TGFβ1 on lymphvasculogenesis (Vittet et al., 2012), our results indicate that BMP9 may counterbalance this TGFβ1 inhibitory action. We also identified a pro-lymphvasculogenic effect for BMP10, the other high affinity ligand for ALK1, to a similar extent to BMP9. On the other hand, and as previously reported (Dunworth et al., 2014), we found a slight but significant inhibition in the formation of LYVE-1-positive cells in response to high BMP2 doses. It thus appears that several members of the TGFβ superfamily play critical roles in early lymphatic endothelial expansion and/or cell specification during mouse ES cell in vitro differentiation.

Concerning the mechanisms and the signaling pathways involved, BrdU incorporation experiments indicate that the stimulation of the proliferation of the early lymphatic-specified LYVE-1-positive cell population contributes to its significant expansion by day 10. Nevertheless, an earlier BMP9 effect could also be involved since we observed that FLK-1+ vascular precursors were direct BMP9 targets, as revealed by the SMAD1/5 protein phosphorylation response experiments. Our results are in accordance with BMP9 effects being in large part mediated by the calcineurin-NFATc1 pathway. A critical role of this pathway is evidenced first by an early increase in *Nfatc1* gene expression in response to the stimulation by 0.3 ng/mL BMP9, and second, by the fact that cyclosporin A, known to block this pathway (Norrmen et al., 2009), reversed the BMP9-induced LYVE-1-positive cell formation during the differentiation of FLK-1+ vascular precursors in co-culture with OP9 stromal cells. Further evidence for an involvement of this pathway is provided at the protein level by the observation of a sustained NFATc1 expression level which may reflect an increased stability or an increased translation ratio of the protein after BMP9 stimulation. The exact mechanism affecting NFATc1 protein remains to be further elucidated in details. The involvement of the calcineurin/NFATc1 signaling pathway in lymphatic development has previously been established (Kulkarni et al., 2009). It was shown that NFATc1 can be observed on some endothelial cells of the cardinal vein that are also positive for PROX-1, at the initial stage of lymphatic fate specification. Later on, it was reported to affect the size of the primary lymph sacs and the patterning and the maintenance of the lymphatic

vasculature, whereas in mature lymphatic endothelial cells, NFATc1 was also reported to induce the expression of certain lymphatic endothelial genes (Kulkarni et al., 2009).

On the other hand, the lack of regulation by BMP9 of the expression of the transcription factors *Coup-tfII*, *Sox18* and *Prox-1*, known to be crucial in the first steps of lymphatic development, indicates that BMP9 probably regulates a population of lymphatic progenitors and/or more distal checkpoints in the commitment of the lymphatic specification. These results are in accordance with the BMP9-induced proliferative effect on an early specified LYVE-1-positive cell population.

Expression analysis during early mouse embryo development demonstrated that BMP9 is detected from E10 (Chen et al., 2013). This timing of expression is compatible with a potential role during lymphatic specification and development that starts at E9.5 for veins or from E12.5 to E13.5 for other embryonic non-venous origins (for review, see (Kazenwadel and Harvey, 2016)). Nonetheless, further experiments remain to be done to fully establish that BMP9 constitutes a key regulator of the initial steps of mouse lymphatic development *in vivo*.

During ES-derived vascular precursor differentiation, high BMP9 concentrations were observed to increase CD31+ LYVE-1- endothelial cell formation. Our data are consistent with an indirect effect relayed by OP9 stromal cells via ALK2 which respond to high BMP9 concentrations by expressing and secreting VEGF-A. Our results provide another evidence, as described in rat mesenchymal stem cells (Ai et al., 2015), that *Vegf-A* constitutes a BMP9 target gene.

This study combined with our previous data (Levet et al., 2013) reveals that BMP9 may act at several different steps of mouse lymphatic endothelial development: first, being pro-lymphvasculogenic during the initiation process, later on regulating the lymphatic vessel maturation and valve formation processes. It should be noted that, during the first steps of lymphatic development, the BMP9 signal intensity appears of great importance in defining the endothelial cell fate of the vascular precursor cells. A potential BMP9 involvement in the regulation of endothelial cell plasticity in adult stages has also been recently discussed (Derynck and Akhurst, 2013; Yoshimatsu et al., 2013). This adds another

level of regulation for BMP9 whose effects appear variable and dependent on the lymphatic maturation stage.

It is currently accepted that BMPs bind to a tetrameric receptor complex composed of two type I and two type II receptors (for review, see (Morrell et al., 2016)). Previous reports have established that BMP9 activates both ALK1 and ALK2 (for review, see (Goumans et al., 2018)). The BMP9 vascular endothelial effects have been in large part linked with the activation of ALK1 whereas its potent osteogenic effect appears mainly mediated by the activation of ALK2 (Garcia de Vinuesa et al., 2016; Lamplot et al., 2013). The endothelial differentiation of adipocyte-derived multipotent cells treated by 10 ng/mL BMP9 was also described to involve ALK2 (Jumabay et al., 2012). In this study, we provide the evidence that the differential BMP9 effects observed, according to dosage, are the consequence of the mobilization of specific type I receptors. Indeed, the RNA silencing experiment results are consistent with the involvement of the ALK1 high affinity BMP9 receptor in the response to low BMP9 doses and of the further mobilization of ALK2 for the high BMP9 concentrations. Interestingly, some recent studies reported that BMP signaling by ALK3 is essential for the zebrafish lymphatic development (Kim and Kim, 2014), and that 10 ng/mL BMP9 activates SMAD1/5 phosphorylation via ALK3 in PA1 breast cancer cells (Varadaraj et al., 2015). Further work then appears necessary to characterize whether ALK3 may also be involved in the endothelial lymphatic effects of BMP9.

The fact that BMP9 constitutes an early driver for the lymphatic lineage expansion during mouse ES cell *in vitro* differentiation appears of great interest to further establish *in vitro* protocols aimed at amplifying lymphatic derivatives from stem cells for cell replacement strategies. However, these data need to be confirmed in human stem cells. Indeed, despite similar responses, such as the negative BMP2 effect on lymphatic differentiation, some differences in BMP signaling between mouse and human ES cells could exist, as described during ES cell self-renewal (for review, see (Li and Chen; 2013)). Some differences in the timing of the events and in the lymphatic fate specification regulating

pathways may also exist, as described between mouse and zebrafish (Koltowska et al., 2015; van Impel et al., 2014).

The generation of lymphatic endothelial cells has already been reported from human ES cells or iPS cells during co-culture experiments with the OP9 murine stromal cell line (Lee et al., 2015). In the light of all our results, the combination of TGFβ and VEGF-A inhibition along with BMP9 stimulation may potentially be particularly useful to expand the lymphatic endothelial cell population. This combination may improve lymphatic differentiation from human stem cells, such as adipose-derived stem cells. Future investigations should be performed in this way since the identification of the basic fundamental mechanisms involved in human lymphvasculogenesis may be of further interest to elaborate novel perspectives of cell therapies for the treatment of lymphedema.

Experimental Procedures:

Cell culture and ES cell differentiation

OP9 stromal cells were obtained from the American Type Culture Collection, Manassas, VA. They were cultured in α-modified Eagle's medium (αMEM) supplemented with 20% FCS and 1% non-essential amino acids, according to the recommendations of the manufacturer.

Murine CJ7 ES cells (Swiatek and Gridley, 1993) (a gift from Dr. T. Gridley, The Jackson Laboratory, Bar Harbor, ME) were used. They were cultured and differentiated into embryoid bodies (EB) as previously described (Prandini et al., 2007; Vittet et al., 2012). EBs were harvested after 5 days of differentiation and were dissociated in non-enzymatic cell dissociation buffer (Life Technologies). After staining with a PE-conjugated rat monoclonal antibody against mouse FLK-1 (BD pharmingen), FLK-1-positive cells were sorted using either a MoFlo FACS cell sorter (DAKO Cytomation, Glostrup, Denmark) or a BD FACS Melody cell sorter (BD Biosciences), and sub-cultured on an OP9 cell stromal feeder layer as previously described (Vittet et al., 2012). When tested, BMPs and other agents were

added at day 6 in serum-free X-vivo15 medium (Lonza Biosciences, Basel, Switzerland). Early lymphatic specification was quantified at day 10 by FACS analysis of LYVE-1-positive cell formation.

Human recombinant BMPs, normal goat IgG (AB-108-C) and neutralizing goat anti-mouse VEGF-A_{164} antibody (AF-493-NA) were purchased from BioTechne. Recombinant human VEGF-A_{165} and human FGF-2 were from PromoCell GmbH, Heidelberg, Germany. All other standard culture reagents were from Life Technologies.

Immunofluorescent stainings

Indirect immunofluorescence experiments on cells cultured in chamber culture slides were performed as previously described (Vittet et al., 2012). The images were acquired using either a ZEISS Axio-Observer Z1 inverted fluorescence microscope and Axiovision 4.8 software, or a ZEISS Axio-Imager 2 fluorescence microscope equipped with an apotome and ZEN software. All images were processed with Adobe Photoshop CS5 software.

Fluorescence activated cell sorting (FACS)

For FACS analysis of endothelial differentiation, cells were detached from the plates using non-enzymatic cell dissociation buffer, as described (Vittet et al., 2012). After two washes with PBS, they were first incubated with LYVE-1 antibody (BioTechne, AF2125) followed by a mixture of PE-conjugated rat anti-mouse CD31 (BD Pharmingen) and Alexa488-conjugated donkey anti-goat antibodies (Jackson ImmunoResearch Laboratories, West Grove, PA). Cells were then analyzed on a FacsCalibur flow cytometer (BD Biosciences) using CellQuest software (BD Biosciences). For CD31+ LYVE-+, CD31+ LYVE-1- and CD31- LYVE-1- cell populations sorting, detached cells from the co-cultures were incubated with a mixture of PE-conjugated rat anti-mouse CD31 and APC-conjugated rat anti-mouse LYVE-1 (BioTechne, FAB2125A).

For the analysis of the proliferative status of cells, co-cultures were pulse labeled with 10 µM BrdU for 1 hour. After cell recovery as described above and first labeling of cell surface LYVE-1 antigens,

the immunofluorescent staining of incorporated BrdU was achieved using the APC BrdU Flow kit (BD Pharmingen) according to the recommended manufacturer's protocol.

Quantitative real-time PCR

In co-culture experiments, confluent layers of OP9 cells were first stained with the long-term fluorescent CellTracker™ Green CMFDA (5-chloromethylfluorescein diacetate) (Molecular Probes, Eugene, OR) before plating FLK-1+ vascular precursors. After 24 hours treatment with 0.3 ng/mL BMP9 in serum-free medium, the CMFDA negative fraction was sorted for gene expression analysis.

For gene expression studies, total RNA was extracted from cells using Nucleospin RNA XS kit (Macherey-Nagel, Düren, Germany) and first strand cDNA was synthesized from 1 µg total RNA by reverse transcription using iScript System (Biorad) according to the manufacturer's instructions. Real time quantitative PCR was performed using a C1000 thermal cycler with a CFX96 real-time PCR detection system (BioRad Laboratories, Hercules, CA) and the ready to use GoTaq QPCR Master Mix (Promega) according to the manufacturer's instructions. Values obtained for each gene were normalized to hypoxanthine phosphoribosyltransferase (HPRT) messenger RNA (mRNA) expression level for relative quantification. The primer sequences used are listed in Table S1.

Protein extraction and Western Blot analysis

Sorted FLK-1+ vascular precursors or OP9 stromal cells were stimulated in suspension in PBS buffer for 1 hour with the different BMP9 concentrations. They were then lysed in RIPA buffer pH 7.4 (50 mM Tris-HCl, 150 mM NaCl, 0.5% desoxycholate, 0.1% SDS, 1 % NP40). Proteins were separated on SDS-PAGE 4-20% gels (BioRad, Mini Protean TGX Stain Free) and immunoblots were performed with rabbit anti-phospho-SMAD1/5 (Cell signaling, 41D10) or mouse anti-NFATc1 (BD Biosciences, clone

7A6) and β-actin (Sigma, AC-15) or GAPDH (Applied Biosystems – Ambion N°AM4300) primary antibodies for the control of protein loading.

VEGF-A Enzyme-linked immunosorbent assay

The VEGF-A levels in the culture medium were measured using a mouse VEGF-A_{164} ELISA kit (BioTechne; Mouse VEGF Quantikine ELISA Kit, MMV00) according to the manufacturer's instructions.

RNA silencing experiments

FLK-1+ vascular precursors in co-culture on OP9 cell layer since 24 hours and adherent OP9 Cells were transfected with 10 nM siRNA using lipofectamine™ RNAiMAX transfection reagent (Life Technologies) according to the manufacturer's instructions. Stimulation with BMP9 was performed 24 hours after transfection, in serum-free medium. In some experiments, FLK-1+ vascular precursors were transfected in cell suspension by improved electroporation using the nucleofector™ technology with the Amaxa device and the optimized protocol developed for stem cells (Lonza). Transfected cells were then plated in co-culture on OP9 stromal cells for 24 hours before stimulation with or without BMP9 for further differentiation study analysis.

siRNAs were purchased from Ambion (*Alk1*, #s986, *Alk2*, #s61924, and siRNA Scramble (*Scr*), AM4613).

Statistics

Values are presented as mean ± SEM. The results were analyzed by unpaired Student's *t* test.

Author Contributions:

M.S., G.M., and D.V. designed and performed research; D.C. took part in the performing of quantitative RT-PCR experiments; V.C-F. performed cell sorting experiments; M.S., J-J.F., S.B. and D.V. discussed the results; D.V. wrote the manuscript with the help of M.S.

Acknowledgments:

The authors thank Mr Stephane Hasse for his participation to the PCR experiments. This research work was supported by Inserm (U1036), CEA (BIG/BCI), UGA, AMRO-HHT France and the Fondation ARC (grant n° PJA 20131200252).

References:

Ai, W.J., Li, J., Lin, S.M., Li, W., Liu, C.Z., and Lv, W.M. (2015). R-smad signaling-mediated VEGF expression coordinately regulates endothelial cell differentiation of rat mesenchymal stem cells. Stem Cells Dev *24*, 1320-1331.

Aspelund, A., Robciuc, M.R., Karaman, S., Makinen, T., and Alitalo, K. (2016). Lymphatic System in Cardiovascular Medicine. Circ Res *118*, 515-530.

Chen, H., Brady Ridgway, J., Sai, T., Lai, J., Warming, S., Roose-Girma, M., Zhang, G., Shou, W., and Yan, M. (2013). Context-dependent signaling defines roles of BMP9 and BMP10 in embryonic and postnatal development. Proc Natl Acad Sci U S A *110*, 11887-11892.

Cunha, S.I., Magnusson, P.U., Dejana, E., and Lampugnani, M.G. (2017). Deregulated TGF-beta/BMP Signaling in Vascular Malformations. Circ Res *121*, 981-999.

David, L., Mallet, C., Mazerbourg, S., Feige, J.J., and Bailly, S. (2007). Identification of BMP9 and BMP10 as functional activators of the orphan activin receptor-like kinase 1 (ALK1) in endothelial cells. Blood *109*, 1953-1961.

Derynck, R., and Akhurst, R.J. (2013). BMP-9 balances endothelial cell fate. Proc Natl Acad Sci U S A *110*, 18746-18747.

Dunworth, W.P., Cardona-Costa, J., Bozkulak, E.C., Kim, J.D., Meadows, S., Fischer, J.C., Wang, Y., Cleaver, O., Qyang, Y., Ober, E.A.*, et al.* (2014). Bone morphogenetic protein 2 signaling negatively modulates lymphatic development in vertebrate embryos. Circ Res *114*, 56-66.

Garcia de Vinuesa, A., Abdelilah-Seyfried, S., Knaus, P., Zwijsen, A., and Bailly, S. (2016). BMP signaling in vascular biology and dysfunction. Cytokine Growth Factor Rev *27*, 65-79.

Goumans, M.J., Zwijsen, A., Ten Dijke, P., and Bailly, S. (2018). Bone Morphogenetic Proteins in Vascular Homeostasis and Disease. Cold Spring Harb Perspect Biol *10*: a022210.

Horsley, V., and Pavlath, G.K. (2002). NFAT: ubiquitous regulator of cell differentiation and adaptation. J Cell Biol *156*, 771-774.

Jakobsson, L., Kreuger, J., and Claesson-Welsh, L. (2007). Building blood vessels--stem cell models in vascular biology. J Cell Biol *177*, 751-755.

Jiang, X., Nicolls, M.R., Tian, W., and Rockson, S.G. (2018). Lymphatic Dysfunction, Leukotrienes, and Lymphedema. Annu Rev Physiol *80*, 49-70.

Jumabay, M., Abdmaulen, R., Urs, S., Heydarkhan-Hagvall, S., Chazenbalk, G.D., Jordan, M.C., Roos, K.P., Yao, Y., and Bostrom, K.I. (2012). Endothelial differentiation in multipotent cells derived from mouse and human white mature adipocytes. J Mol Cell Cardiol *53*, 790-800.

Kazenwadel, J., and Harvey, N.L. (2016). Morphogenesis of the lymphatic vasculature: A focus on new progenitors and cellular mechanisms important for constructing lymphatic vessels. Dev Dyn *245*, 209-219.

Kim, J.D., and Kim, J. (2014). Alk3/Alk3b and Smad5 mediate BMP signaling during lymphatic development in zebrafish. Mol Cells *37*, 270-274.

Koltowska, K., Lagendijk, A.K., Pichol-Thievend, C., Fischer, J.C., Francois, M., Ober, E.A., Yap, A.S., and Hogan, B.M. (2015). Vegfc Regulates Bipotential Precursor Division and Prox1 Expression to Promote Lymphatic Identity in Zebrafish. Cell Rep *13*, 1828-1841.

Kono, T., Kubo, H., Shimazu, C., Ueda, Y., Takahashi, M., Yanagi, K., Fujita, N., Tsuruo, T., Wada, H., and Yamashita, J.K. (2006). Differentiation of lymphatic endothelial cells from embryonic stem cells on OP9 stromal cells. Arterioscler Thromb Vasc Biol *26*, 2070-2076.

Kreuger, J., Nilsson, I., Kerjaschki, D., Petrova, T., Alitalo, K., and Claesson-Welsh, L. (2006). Early lymph vessel development from embryonic stem cells. Arterioscler Thromb Vasc Biol *26*, 1073-1078.

Kulkarni, R.M., Greenberg, J.M., and Akeson, A.L. (2009). NFATc1 regulates lymphatic endothelial development. Mech Dev *126*, 350-365.

Lamplot, J.D., Qin, J., Nan, G., Wang, J., Liu, X., Yin, L., Tomal, J., Li, R., Shui, W., Zhang, H.*, et al.* (2013). BMP9 signaling in stem cell differentiation and osteogenesis. Am J Stem Cells *2*, 1-21.

Lee, S.J., Park, C., Lee, J.Y., Kim, S., Kwon, P.J., Kim, W., Jeon, Y.H., Lee, E., and Yoon, Y.S. (2015). Generation of pure lymphatic endothelial cells from human pluripotent stem cells and their therapeutic effects on wound repair. Sci Rep *5*, 11019. doi: 10.1038/srep11019.

Levet, S., Ciais, D., Merdzhanova, G., Mallet, C., Zimmers, T.A., Lee, S.J., Navarro, F.P., Texier, I., Feige, J.J., Bailly, S.*, et al.* (2013). Bone morphogenetic protein 9 (BMP9) controls lymphatic vessel maturation and valve formation. Blood *122*, 598-607.

Liersch, R., Nay, F., Lu, L., and Detmar, M. (2006). Induction of lymphatic endothelial cell differentiation in embryoid bodies. Blood *107*, 1214-1216.

Ma, W., and Oliver, G. (2017). Lymphatic Endothelial Cell Plasticity in Development and Disease. Physiology *32*, 444-452.

Matsumura, K., Hirashima, M., Ogawa, M., Kubo, H., Hisatsune, H., Kondo, N., Nishikawa, S., and Chiba, T. (2003). Modulation of VEGFR-2-mediated endothelial-cell activity by VEGF-C/VEGFR-3. Blood *101*, 1367-1374.

Morrell, N.W., Bloch, D.B., ten Dijke, P., Goumans, M.J., Hata, A., Smith, J., Yu, P.B., and Bloch, K.D. (2016). Targeting BMP signalling in cardiovascular disease and anaemia. Nat Rev Cardiol *13*, 106-120.

Murtomaki, A., Uh, M.K., Choi, Y.K., Kitajewski, C., Borisenko, V., Kitajewski, J., and Shawber, C.J. (2013). Notch1 functions as a negative regulator of lymphatic endothelial cell differentiation in the venous endothelium. Development *140*, 2365-2376.

Niessen, K., Zhang, G., Ridgway, J.B., Chen, H., and Yan, M. (2010). ALK1 signaling regulates early postnatal lymphatic vessel development. Blood *115*, 1654-1661.

Norrmen, C., Ivanov, K.I., Cheng, J., Zangger, N., Delorenzi, M., Jaquet, M., Miura, N., Puolakkainen, P., Horsley, V., Hu, J.*, et al.* (2009). FOXC2 controls formation and maturation of lymphatic collecting vessels through cooperation with NFATc1. J Cell Biol *185*, 439-457.

Prandini, M.H., Desroches-Castan, A., Feraud, O., and Vittet, D. (2007). No evidence for vasculogenesis regulation by angiostatin during mouse embryonic stem cell differentiation. J Cell Physiol *213*, 27-35.

Qi, S., and Pan, J. (2015). Cell-based therapy for therapeutic lymphangiogenesis. Stem Cells Dev *24*, 271-283.

Rostama, B., Turner, J.E., Seavey, G.T., Norton, C.R., Gridley, T., Vary, C.P., and Liaw, L. (2015). DLL4/Notch1 and BMP9 Interdependent Signaling Induces Human Endothelial Cell Quiescence via P27KIP1 and Thrombospondin-1. Arterioscler Thromb Vasc Biol *35*, 2626-2637.

Scharpfenecker, M., van Dinther, M., Liu, Z., van Bezooijen, R.L., Zhao, Q., Pukac, L., Lowik, C.W., and ten Dijke, P. (2007). BMP-9 signals via ALK1 and inhibits bFGF-induced endothelial cell proliferation and VEGF-stimulated angiogenesis. J Cell Sci *120*, 964-972.

Semo, J., Nicenboim, J., and Yaniv, K. (2016). Development of the lymphatic system: new questions and paradigms. Development *143*, 924-935.

Shaitelman, S.F., Cromwell, K.D., Rasmussen, J.C., Stout, N.L., Armer, J.M., Lasinski, B.B., and Cormier, J.N. (2015). Recent progress in the treatment and prevention of cancer-related lymphedema. CA Cancer J Clin *65*, 55-81.

Sieber, C., Kopf, J., Hiepen, C., and Knaus, P. (2009). Recent advances in BMP receptor signaling. Cytokine Growth Factor Rev *20*, 343-355.

Suzuki, Y., Ohga, N., Morishita, Y., Hida, K., Miyazono, K., and Watabe, T. (2010). BMP-9 induces proliferation of multiple types of endothelial cells in vitro and in vivo. J Cell Sci *123*, 1684-1692.

Swiatek, P.J., and Gridley, T. (1993). Perinatal lethality and defects in hindbrain development in mice homozygous for a targeted mutation of the zinc finger gene Krox20. Genes Dev *7*, 2071-2084.

Toyserkani, N.M., Christensen, M.L., Sheikh, S.P., and Sorensen, J.A. (2015). Stem cells show promising results for lymphoedema treatment--a literature review. J Plast Surg and Hand Surg *49*, 65-71.

van Impel, A., Zhao, Z., Hermkens, D.M., Roukens, M.G., Fischer, J.C., Peterson-Maduro, J., Duckers, H., Ober, E.A., Ingham, P.W., and Schulte-Merker, S. (2014). Divergence of zebrafish and mouse lymphatic cell fate specification pathways. Development *141*, 1228-1238.

Varadaraj, A., Patel, P., Serrao, A., Bandyopadhay, T., Lee, N.Y., Jazaeri, A.A., Huang, Z., Murphy, S.K., and Mythreye, K. (2015). Epigenetic Regulation of GDF2 Suppresses Anoikis in Ovarian and Breast Epithelia. Neoplasia *17*, 826-838.

Vittet, D., Merdzhanova, G., Prandini, M.H., Feige, J.J., and Bailly, S. (2012). TGFbeta1 inhibits lymphatic endothelial cell differentiation from mouse embryonic stem cells. J Cell Physiol *227*, 3593-3602.

Yoshimatsu, Y., Lee, Y.G., Akatsu, Y., Taguchi, L., Suzuki, H.I., Cunha, S.I., Maruyama, K., Suzuki, Y., Yamazaki, T., Katsura, A.*, et al.* (2013). Bone morphogenetic protein-9 inhibits lymphatic vessel formation via activin receptor-like kinase 1 during development and cancer progression. Proc Natl Acad Sci U S A *110*, 18940-18945.

LEGENDS OF FIGURES

Figure 1: *ES-derived vascular precursors co-cultured on murine stromal OP9 cells are able to form early lymphatic derivatives*. A) Schematic of the differentiation protocol illustrating the main steps and specific treatments according to the experiment goals. B) Morphological observations of endothelial cell clusters formed after 5 days of co-culture (day 10 of differentiation) in control conditions. The arrows point to cell clusters exhibiting an endothelial-like morphology. C to G) Immunofluorescence stainings of endothelial cell-like clusters obtained in unstimulated control conditions at day 10/11 with anti-CD31 (C), anti-LYVE-1 (D, G) and anti-PROX-1 (F) antibodies. Nuclei were counterstained with Hoechst 33258 (C, E). Scale bars for all panels: 100 µm. H) Flow cytometry dot plot of the LYVE-1 and CD31 double immunostaining of the co-cultures at day10/11 used for cell sortings. The different gates used are outlined: R1, CD31+/LYVE-1+ cells; R2, CD31+/LYVE-1- cells; R3, CD31-/LYVE-1- cells. To obtain sufficient cell numbers in the LYVE-1+ and LYVE-1- cell fraction, cocultures were performed in the presence of 0.3 ng/ml BMP9. I) Data are the mean value ± SD of triplicates from the quantitative RT-PCR experiment performed with the RNAs extracted from the different cell populations gated on the dot plot of the experiment illustrated in H. See also Figure S1.

Figure 2: *BMP9 increases the formation of LYVE-1+ cells during the co-culture of ES-derived vascular precursors on murine stromal OP9 cells*. A) Flow cytometry analysis of the formation of LYVE-1+ early lymphatic-specified endothelial cells from co-cultures of FLK-1+ vascular precursors on OP9 stromal cells, in response to variable concentrations of BMPs. Vascular precursors were plated on OP9 stromal cells at day 5, and BMPs were added under serum-free conditions after 24h of co-culture. The formation of LYVE-1-positive cells was measured at day 10 (after 4 days of stimulation with BMPs). Data are the mean ± SEM of 4 (BMP2), 8 (BMP10) or 11 (BMP9) different experiments. *** $P < 0.001$; ** $P < 0.01$; * $P < 0.05$, significantly different from basal control values using unpaired Student's t -test. B) Schematic of the differentiation kinetics protocol with the different time points

used for pulse labeling with BrdU. C) Flow cytometry analysis of the formation of LYVE-1-positive cells in the absence (CTL) or in the presence of 0.3 ng/mL BMP9 added at day 6. The reported data originated from pooled different experiments. They are the mean values ± SEM obtained from 2 (Day6), 5 (Day7 and Day8), and 8 (Day10/11)) different set of values, according to the considered time point. *** $P < 0.001$, significantly different from its respective control using unpaired Student's t –test. D) Representative flow cytometry charts of pulse BrdU labeling of the co-cultures after 24 hours (Day 7) and 48 hours (Day 8) without (CTL) or after BMP9 (0.3 ng/mL) stimulation. The upper dot plots illustrated the LYVE-1 cells immunoreactivity (LYVE-1 positive cells are gated in R2); and the lower histogram plots showed the BrdU immunoreactivity of the R2-gated LYVE-1 positive cell population. The percentage of positive cells are indicated on each plot. The BMP9 fold stimulation of BrdU incorporation in LYVE-1 positive cells is reported in the right histogram chart and represented the mean ± SD of 2 independent experiments. See also Figure S2.

Figure 3: *Low concentrations of BMP9 modulates the calcineurin/NFATc1 signaling pathway.* A) Quantitative RT-PCR analysis of BMP9 effects on the mRNA levels of transcription factors known to be essential for lymphatic differentiation. FLK-1+ vascular precursors at day 5 were plated on CellTracker CMFDA-stained OP9 stromal cells. BMP9 (0.3 ng/mL) was added at day 6. After 24h of treatment, the CMFDA-negative cell population was sorted and collected for gene expression analysis. Data are the mean ± SEM of 5 experiments. B) NFATc1 protein expression analysis after BMP9 stimulation. FLK-1+ vascular precursors at day 5 were stimulated in suspension in serum-free medium with or without 0.3 ng/mL BMP9 for 20 min. Immunoblotting was performed using an antibody against NFATc1 or actin proteins as a loading control. Results of a representative experiment, out of 3, are illustrated. Sizes of the molecular weight markers are indicated on the left. C) Inhibition of NFATc1 signaling by cyclosporin A prevents the BMP9-induced increase in LYVE-1+ cell formation. LYVE-1-positive cell formation was measured by flow cytometry 4 days after addition

of BMP9 in the absence or in the presence of cyclosporin A. Data are the mean ± SEM of 3 experiments.

* P < 0.05, significantly different from control untreated cells (A) and significantly different from treatment with BMP9 alone (B) using unpaired Student's t -test. See also Figure S3.

Figure 4: *Analysis of CD31+ LYVE-1- endothelial cell formation during the co-culture of ES-derived vascular precursors on murine stromal OP9 cells*. A) Flow cytometry quantitative measurement of CD31+ LYVE-1- cell formation after co-culture of FLK-1+ vascular precursors on OP9 stromal cells in response to variable concentrations of BMP9. Data are the mean ± SEM of 4 (BMP2), 8 (BMP10) or 11 (BMP9) different experiments. * P < 0.05, significantly different from basal control values using unpaired Student's t-test. B) Immunofluorescence staining with anti-CD31 and anti-LYVE-1 antibodies of cell co-cultures at day 10 of differentiation, in the absence (CTL) or in the presence of 10 ng/mL BMP9. Scale bar for each panel: 200 µm.

Figure 5: *VEGF-A regulates endothelial differentiation from ES-derived vascular precursors and mediates the effects of high BMP9 concentrations.* A) Quantitative flow cytometry analysis of the formation of CD31+ LYVE-1- and CD31+ LYVE-1+ cells in response to variable doses of VEGF-A. Data are the mean ± SEM of 5 different experiments. B) Dose-dependent VEGF-A effects on the formation of CD31 positive endothelial cells (blue line) and on their repartition between LYVE-1+ early-lymphatic specified (green bars) and LYVE-1- (red bars) endothelial cells. Data are the means ± SEM from 5 or 6 experiments C) VEGF-A production in the co-culture differentiation medium. VEGF-A levels were measured by ELISA after 48h of treatment with the indicated agents. Values are the mean ± SD values from 2 to 3 experiments. D) Anti-VEGF-A neutralizing antibody inhibits control and BMP9-induced CD31+ LYVE-1- cell formation from ES-derived vascular precursors in co-culture on

OP9 stromal cells. Data are the mean ± SEM of 5 experiments. E) BMP9 functional coupling with SMAD1/5 phosphorylation in OP9 stromal cells. Serum-starved sub-confluent OP9 cells were stimulated 1 hour in the absence (CTL) or in the presence of variable BMP9 concentrations. Immunoblots with phospho SMAD1/5 antibodies and actin antibodies for normalization are illustrated. F) Effects of 10 ng/mL BMP9 on VEGF-A production by OP9 cells. Data are the mean ± SEM of 7 experiments. * P < 0.05; ** P < 0.01, *** P < 0.001, significantly different from respective controls or as indicated, using unpaired Student's t-test.

Figure 6: *Analysis of differential BMP type I receptor involvement in the BMP9 low dose and high dose effects by RNA silencing experiments.* A) Effect of *Alk1* and *Alk2* siRNA on LYVE-1 positive cell formation induced by 0.3 ng/mL BMP9 in FLK-1+ vascular precursors co-cultures on mouse OP9 cells. *Alks* knockdown were performed by siRNA transfection of vascular precursors by either electroporation or by using lipofectamine RNAimax, 24 hours before BMP9 stimulation. Data are the mean ± SEM of 3 (si*Alk2*) or 4 (si*Scr*, si*Alk1*) different experiments. B) High dose BMP9-induced LYVE-1- endothelial cell formation is inhibited after prior *Alk2* knockdown in OP9 cells. OP9 cells were first transfected by lipofectamine RNAimax with the different siRNA, 24 hours before FLK-1+ vascular precursors plating in co-culture on OP9 cells, and 48 hours before stimulation with 10 ng/mL BMP9. LYVE-1-negative CD31-positive cell formation is illustrated. Data are the mean ± SEM of 3 experiments. C, D) *Alk2* knockdown in OP9 cells prevents SMAD1/5 phosphorylation and VEGF-A secretion induced by 10 ng/mL BMP9. OP9 cells were transfected with the different siRNA by lipofectamine RNAimax, 48 hours before stimulation with 10 ng/mL BMP9. For SMAD1/5 phosphorylation studies, serum-starved sub-confluent OP9 cells were stimulated 1 hour in the absence (CTL) or in the presence of BMP9, before immunoblotting with anti P-SMAD1/5 and actin antibodies (C). VEGF-A levels were measured after 48 hours of treatment with or without 10 ng/mL BMP9, by ELISA (D). Data are mean ± SEM of 3 experiments. * P < 0.05, *** P < 0.001, significantly

different from BMP9 stimulation obtained after transfection with siScramble (si*Scr*), using unpaired Student's t-test. See also Figure S4.

Figure 7: *Hypothetical model for BMP9 regulation of ES-derived vascular precursor differentiation in co-culture with murine OP9 stromal cells.*

Low BMP9 concentrations induce the formation of LYVE-1+ early lymphatic-specified endothelial cells through ALK1 activation. BMP9 was observed to directly activate FLK-1+ vascular precursors and earlier stages of vascular committed cells through mobilization of the NFATc1 signaling pathway. Moreover, an increase in the proliferation of the LYVE-1-positive cell population was found to largely contribute to its expansion. At higher doses, BMP9 could, in addition to ALK1, also activates ALK2 present on OP9 stromal cells. This leads to a significant rise in the secretion of VEGF-A by OP9 cells, with as a resultant effect, an increase in LYVE-1- endothelial cell population at the expense of the LYVE-1+ early lymphatic-specified endothelial cell formation.

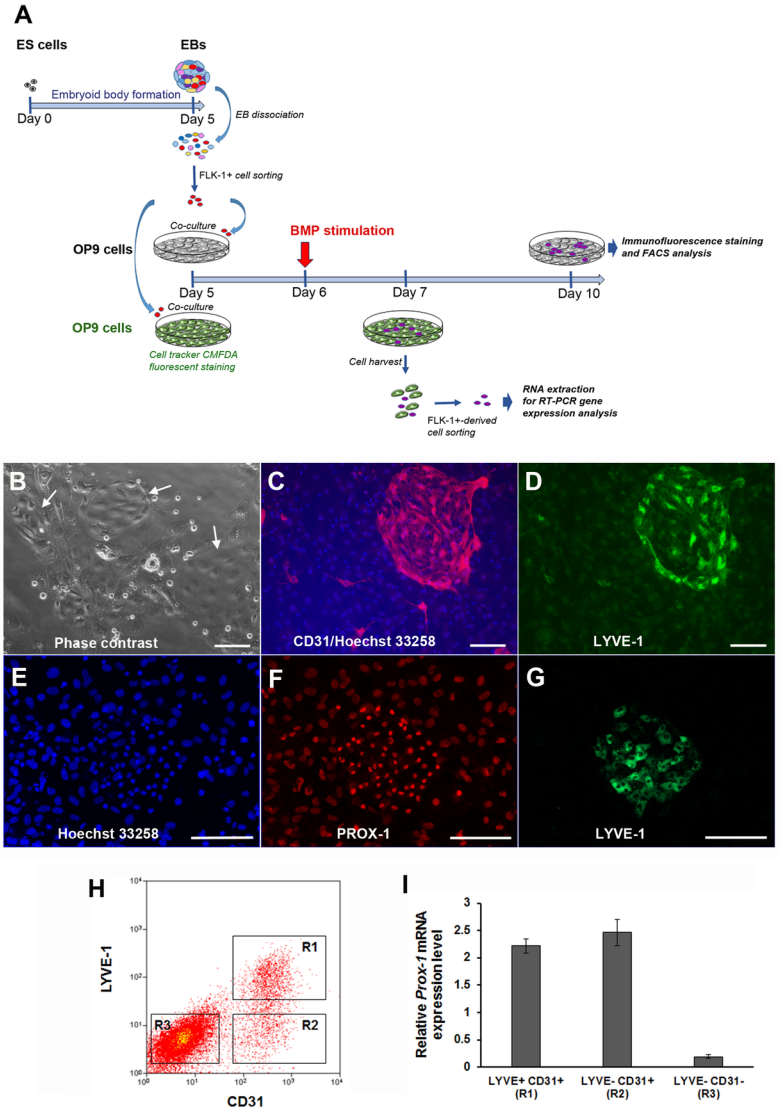
A
ES cells
EBs
Embryoid body formation
Day 0
Day 5
EB dissociation
FLK-1+ cell sorting
Co-culture
OP9 cells
BMP stimulation
Immunofluorescence staining and FACS analysis
Day 5
Day 6
Day 7
Day 10
Co-culture
OP9 cells
Cell tracker CMFDA fluorescent staining
Cell harvest
RNA extraction for RT-PCR gene expression analysis
FLK-1+-derived cell sorting
B
Phase contrast
C
CD31/Hoechst 33258
D
LYVE-1
E
Hoechst 33258
F
PROX-1
G
LYVE-1
H
LYVE-1
CD31
R1
R2
R3
I
Relative Prox-1 mRNA expression level
LYVE+ CD31+ (R1)
LYVE- CD31+ (R2)
LYVE- CD31- (R3)

Figure 1

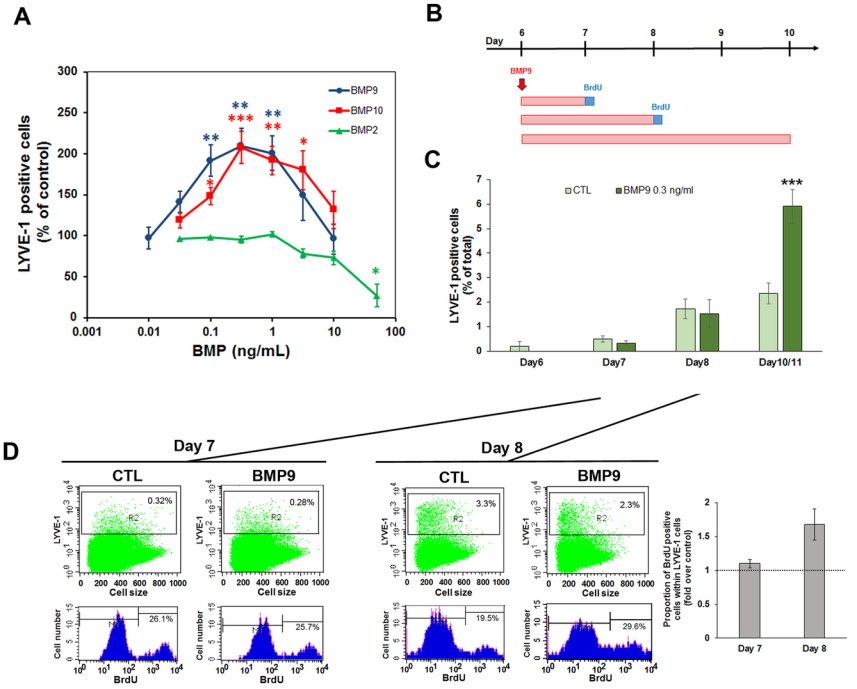
A
LYVE-1 positive cells (% of control)
BMP (ng/mL)
BMP9
BMP10
BMP2
B
Day
BMP9
BrdU
BrdU
C
LYVE-1 positive cells (% of total)
CTL
BMP9 0.3 ng/ml
Day6
Day7
Day8
Day10/11
D
Day 7
Day 8
CTL
BMP9
CTL
BMP9
LYVE-1
Cell size
Cell number
BrdU
0.32%
0.28%
3.3%
2.3%
26.1%
25.7%
19.5%
29.6%
Proportion of BrdU positive cells within LYVE-1 cells (fold over control)
Day 7
Day 8

Figure 2

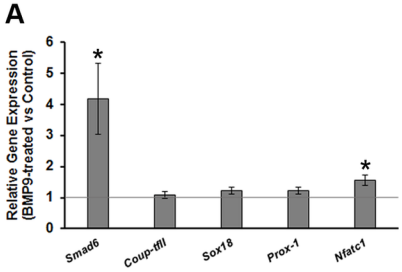
A
Relative Gene Expression (BMP9-treated vs Control)
6
5
4
3
2
1
0
*
*
Smad6
Coup-tfII
Sox18
Prox-1
Nfatc1

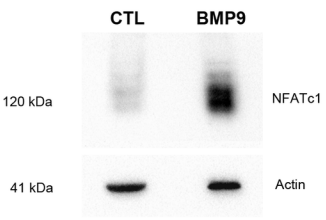
B
CTL
BMP9
120 kDa
NFATc1
41 kDa
Actin

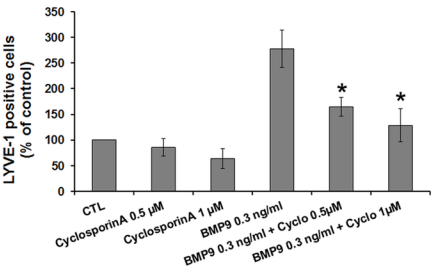
C
LYVE-1 positive cells (% of control)
350
300
250
200
150
100
50
0
*
*
CTL
CyclosporinA 0.5 µM
CyclosporinA 1 µM
BMP9 0.3 ng/ml
BMP9 0.3 ng/ml + Cyclo 0.5µM
BMP9 0.3 ng/ml + Cyclo 1µM

Figure 3

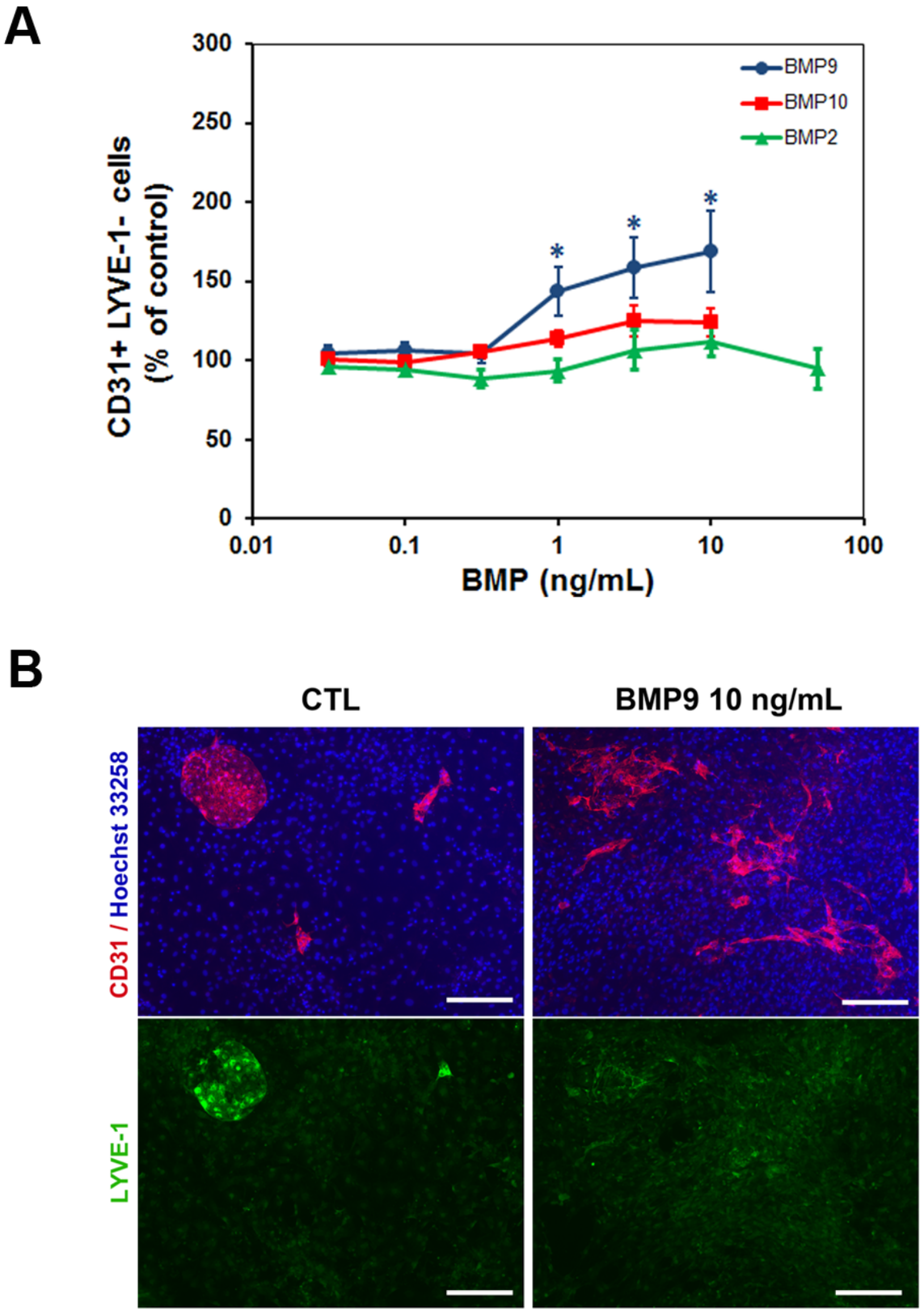
A
300
250
200
150
100
50
0
CD31+ LYVE-1- cells
(% of control)
BMP9
BMP10
BMP2
*
*
*
0.01
0.1
1
10
100
BMP (ng/mL)
B
CTL
BMP9 10 ng/mL
CD31 / Hoechst 33258
LYVE-1

Figure 4

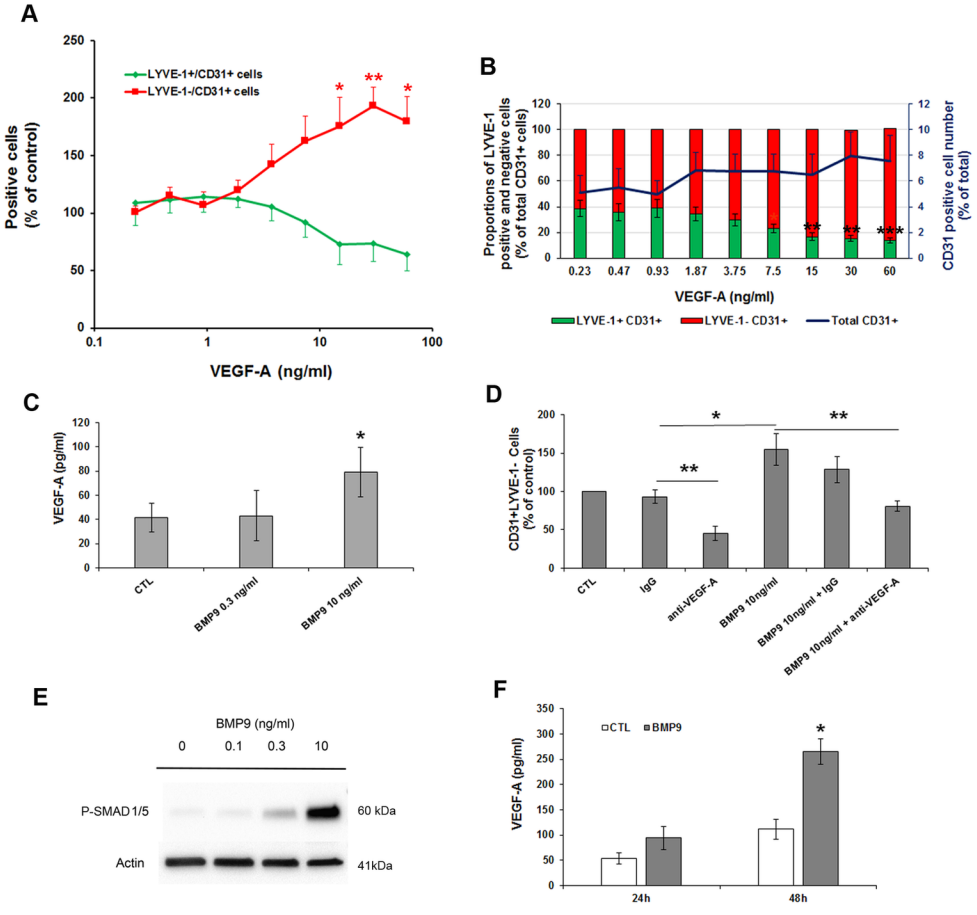
A
Positive cells (% of control)
LYVE-1+/CD31+ cells
LYVE-1-/CD31+ cells
VEGF-A (ng/ml)
B
Proportions of LYVE-1 positive and negative cells (% of total CD31+ cells)
CD31 positive cell number (% of total)
VEGF-A (ng/ml)
LYVE-1+ CD31+
LYVE-1- CD31+
Total CD31+
C
VEGF-A (pg/ml)
CTL
BMP9 0.3 ng/ml
BMP9 10 ng/ml
D
CD31+LYVE-1- Cells (% of control)
CTL
IgG
anti-VEGF-A
BMP9 10ng/ml
BMP9 10ng/ml + IgG
BMP9 10ng/ml + anti-VEGF-A
E
BMP9 (ng/ml)
0
0.1
0.3
10
P-SMAD1/5
60 kDa
Actin
41kDa
F
CTL
BMP9
VEGF-A (pg/ml)
24h
48h

Figure 5

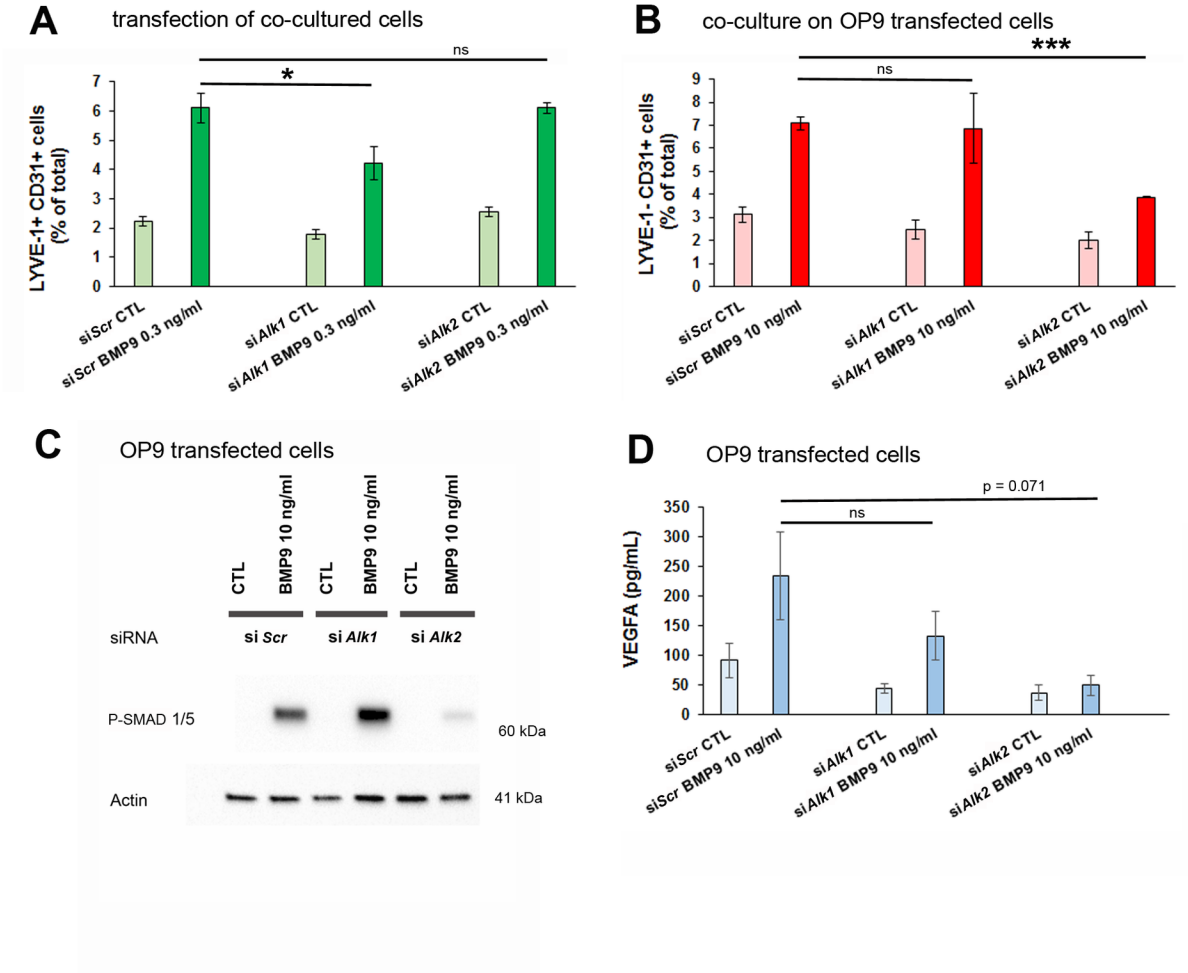
A
transfection of co-cultured cells
ns
*
LYVE-1+ CD31+ cells (% of total)
siScr CTL
siScr BMP9 0.3 ng/ml
siAlk1 CTL
siAlk1 BMP9 0.3 ng/ml
siAlk2 CTL
siAlk2 BMP9 0.3 ng/ml
B
co-culture on OP9 transfected cells
***
ns
LYVE-1- CD31+ cells (% of total)
siScr CTL
siScr BMP9 10 ng/ml
siAlk1 CTL
siAlk1 BMP9 10 ng/ml
siAlk2 CTL
siAlk2 BMP9 10 ng/ml
C
OP9 transfected cells
CTL
BMP9 10 ng/ml
siRNA
si Scr
si Alk1
si Alk2
P-SMAD 1/5
60 kDa
Actin
41 kDa
D
OP9 transfected cells
p = 0.071
ns
VEGFA (pg/mL)
siScr CTL
siScr BMP9 10 ng/ml
siAlk1 CTL
siAlk1 BMP9 10 ng/ml
siAlk2 CTL
siAlk2 BMP9 10 ng/ml

Figure 6

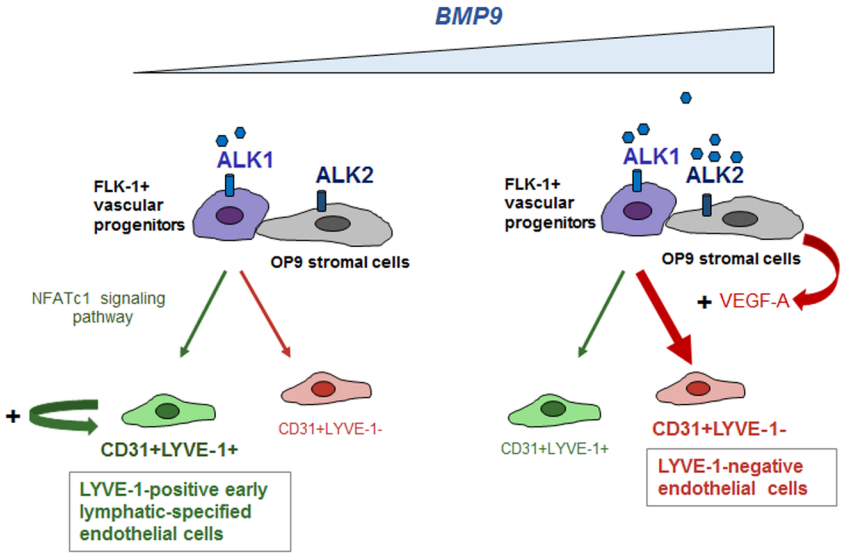
BMP9
ALK1
ALK2
FLK-1+
vascular
progenitors
OP9 stromal cells
NFATc1 signaling
pathway
+
CD31+LYVE-1+
CD31+LYVE-1-
LYVE-1-positive early
lymphatic-specified
endothelial cells
ALK1
ALK2
FLK-1+
vascular
progenitors
OP9 stromal cells
+ VEGF-A
CD31+LYVE-1+
CD31+LYVE-1-
LYVE-1-negative
endothelial cells

Figure 7